

Wear-Resistant Oxide Coatings on Aluminum Alloy Formed in Borate and Silicate Aqueous Electrolytes by Plasma Electrolytic Oxidation

V. S. Rudnev^{a, b, *}, T. P. Yarovaya^a, P. M. Nedozorov^a, and Yu. N. Mansurov^b

^a Institute of Chemistry, Far-Eastern Branch, Russian Academy of Sciences, Vladivostok, 690022 Russia

^b Far Eastern Federal University, Vladivostok, 690950 Russia

*e-mail: rudnevvs@ich.dvo.ru

Received February 17, 2016

Abstract—There are several methods known of formation of wear-resistant oxide coatings on articles made of aluminum alloys by the method of plasma electrolytic oxidation (PEO), for example, in silicate and borate aqueous electrolytes. In the present work, a comparison of characteristics of PEO coatings obtained on AMg5 and D16 aluminum alloys in the bipolar mode by these two methods, as well as in mixed borate–silicate electrolytes, has been performed.

DOI: 10.1134/S2070205117030200

1. INTRODUCTION

Plasma electrolytic oxidation (PEO) of valve metals and alloys (Al, Mg, Ti, Zr, Nb, etc.) comprises the development of a traditional method of electrochemical anodization [1–20]. The latter has been extensively used in industry for finishing articles made of aluminum and its alloys; their preparation prior to deposition of paints, lacquers, and polymers; and protection from corrosion and mechanical destruction. PEO is distinguished from the traditional anodization by the performance of the process in electrolytes and under electric voltages that allow creation of an ensemble (manifold) of electric microbreakdowns on the surface of the growing oxide layer, i.e., carrying out anodization (oxide-coating growth) under conditions of an additional impact of spark or arc electric discharges on the growing oxide, see Fig. 1. These conditions (a) increase the coating-growth rate through increasing the mass transfer, as well as by involving electrolyte components into the coating formation, (b) create fast-cooling (the aqueous electrolyte temperature is close to room temperature) micromelts of the oxide material, and (c) allow initiating as the formation of specific chemical compounds in coatings as crystallization of oxide phases. All the above factors extend significantly the possibilities of the method of anodization of metals and alloys in aqueous electrolytes with respect to both composition and structure of the formed coatings as to their functional features.

Some directions of advanced studies in the field of application of coatings formed on valve metals by the PEO method are shown in the diagram in Fig. 2 [19, 20]. The main mechanisms of coating growth under

the effect of different types of surface electric discharges and breakdowns, as well as approaches developed to the preparation of electrolytes to be used in the formation of coatings of specific oxide compositions, were partially summarized in [21, 22].

PEO enables one to form coatings with a solid layer of wear-resistant phases of aluminum oxides (α -, γ -Al₂O₃) on aluminum and its alloys [2, 4–6, 11, 12, 16–18, 23–26], which is virtually unattainable by other methods. The method of formation of wear-resistant coatings in an alkaline silicate electrolyte by the bipolar anode–cathode current was suggested for the first time by G.A. Markov and colleagues of his in Novosibirsk [4, 11, 23]. Due to its simplicity and technological features, this method has been applied extensively in our country and abroad.

Recently, an alternative method based on application of borate electrolytes (aqueous solutions of alkali metal borates) has been suggested [6, 25, 26]. It appears of interest to compare the above two methods with respect to technological formation parameters and coating composition and structure and to reveal whether the coating formation in mixed borate–silicate electrolytes would produce a synergetic improvement of their useful wear-resistance properties.

2. MATERIALS AND METHODS

2.1. Composition of Aluminum Alloys

Coatings were formed on samples made of aluminum alloys of grades AMg5 and D16 of a thickness of ~1 mm. The alloys element composition is shown in Table 1. Samples with a size of 40 × 40 and 10 × 40 mm

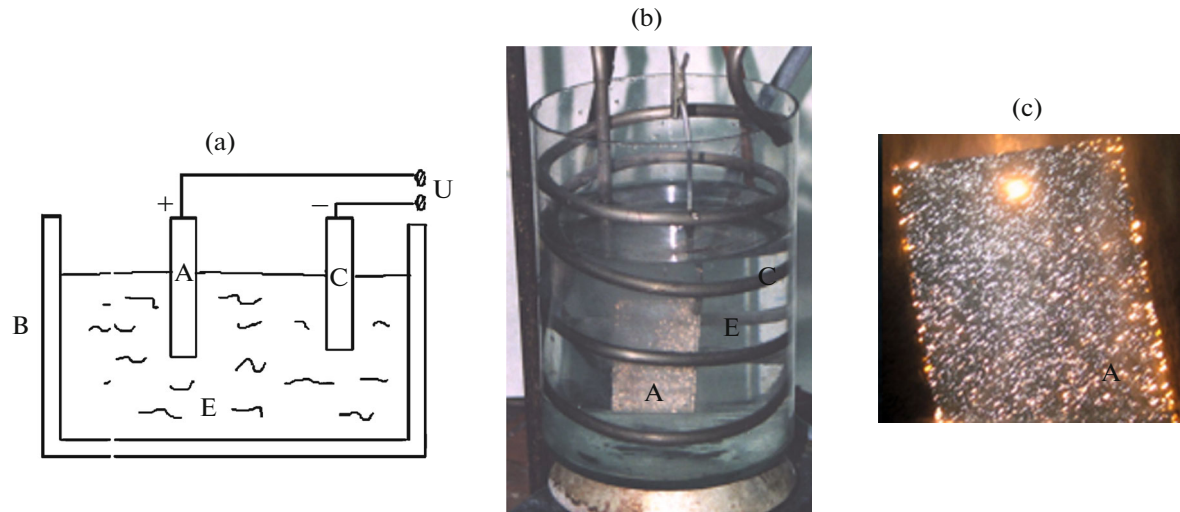


Fig. 1. Scheme of the cell for plasma electrolytic oxidation: B, bath with cooling jacket with flowing tap water; E, aqueous electrolyte; A and C, anode and cathode, respectively; U , potential difference on electrodes (a). General appearance of the cell with electrolyte and the anode surface with electric-spark discharges at the anode–electrolyte interface (b). Spark discharges on the anode surface (c).

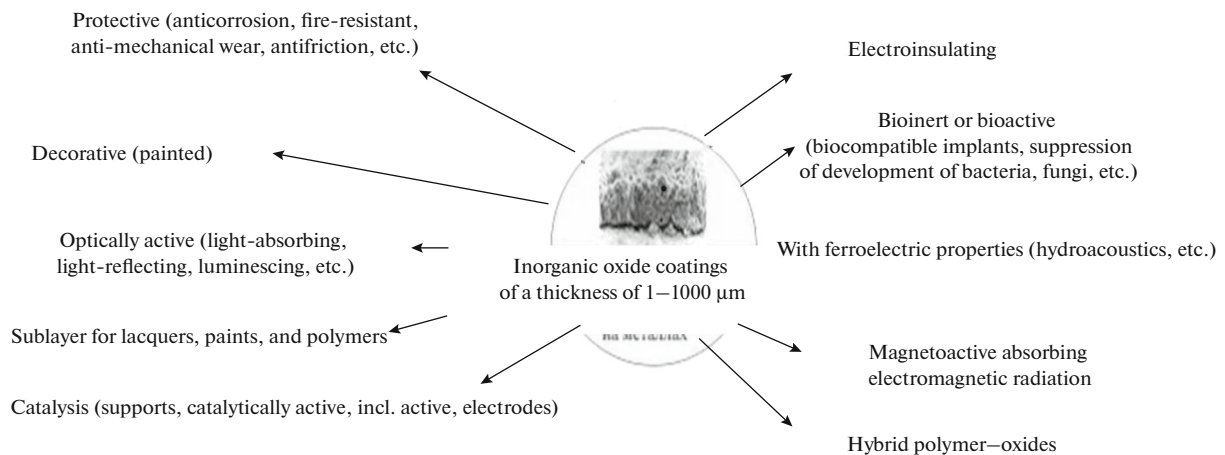


Fig. 2. [19, 20] Some advanced directions in fabrication of functional coatings by the method of plasma electrolytic oxidation on the surface of valve metals and alloys.

were cut using a guillotine. Prior to oxidation, samples underwent mechanical treatment in order to obtain rounded corners and remove rough edges. Thereafter, samples were chemically polished in a solution of concentrated $\text{H}_3\text{PO}_4(\text{c}) + \text{H}_2\text{SO}_4(\text{c}) + \text{HNO}_3(\text{c})$ acids at a ratio of 4 : 2 : 1 at 80–90°C for 5–10 s. Upon chemical polishing, samples were washed in tap and distilled water and dried in air.

2.2. Electrolytes

Two base electrolytes were used: no. 1, 20 g/L $\text{K}_2\text{B}_4\text{O}_7 \cdot 4\text{H}_2\text{O}$, and no. 2, 10 g/L $\text{Na}_2\text{SiO}_3 \cdot 9\text{H}_2\text{O} + 2 \text{ g/L KOH}$. All reagents were of chemically pure grade. Electrolytes were prepared by dissolution of

respective salts in distilled water under intensive stirring. The mixed electrolytes of a composition of 20 g/L $\text{K}_2\text{B}_4\text{O}_7 + (10 \text{ g/L Na}_2\text{SiO}_3 \cdot 9\text{H}_2\text{O} + 2 \text{ g/L KOH})$ were prepared through mixing base electrolytes at 1 : 3, 1 : 1, and 3 : 1 immediately prior to experiments.

2.3. Plasma Electrolytic Oxidation Cell

The cell (Figs. 1a, 3) consisted of steel bath 1 with water cooling jacket 2 into which the electrolyte was poured. The bath frame served as a counterelectrode. Electrolyte stirring was carried out using mechanical stirrer 4. The current through the cell, just like the potential difference on electrodes, were set and controlled by a computer. The electrolyte temperature was

Table 1. Element composition of aluminum alloys

Alloy	Impurities, % (not higher than), remaining part Al								
	Fe	Si	Cu	Mn	Ti	Mg	Zn	Ni	other
D16	up to 0.5	up to 0.5	3.8–4.9	0.3–0.9	up to 0.15	1.2–1.8	up to 0.25	up to 0.1	0.05–0.15
AMg5	up to 0.5	up to 0.5	up to 0.1	0.5–0.8	0.02–0.1	4.8–5.8	0.2	N/A	0.1

measured using thermometer 5. To cool the electrolyte, cold tap water was pumped through the bath jacket. In the experiments, the electrolyte temperature did not exceed 30°C. Computer-controlled reverse TER-63/4460N thyristor device (Russia) 6 operating in both unipolar and bipolar anode–cathode modes was used as a current source. Coatings on samples were formed in the anode–cathode mode at effective densities of anode and cathode currents of 0.15 A/cm² and durations of pulses of respective currents of 0.02 s for 120 min. Upon treatment, the samples with coatings were washed with tap and distilled water and dried in air at 70°C.

2.4. Determination of Coating Phase and Element Composition

The coating phase composition was determined using a D8 ADVANCE diffractometer (Germany) in CuK_α-radiation. To analyze X-ray images, the EVA search program with the PDF-2 database was used. The coating element composition was determined using a JXA-8100 X-ray spectral analyzer (JEOL, Japan) with an INCA-sight energy-dispersive accessory (Oxford Instruments, United States). The accessory enables one to perform quantitative element analysis of samples in a “point” of a diameter of about 1 μm (with stationary probing electron beam) by scanning specific areas on the sample surface, to obtain surface images, and to construct maps of element distribution over the sample area and profiles of elements distribution over the sample surface and cross section.

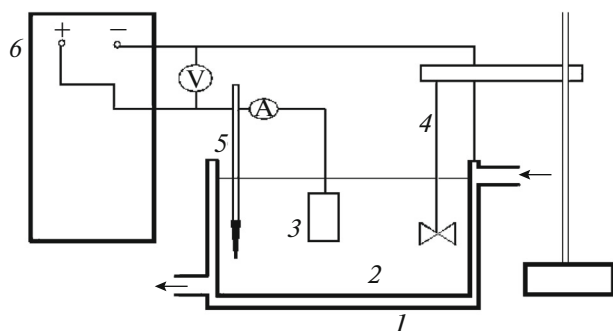


Fig. 3. Scheme of the installation for sample anodization: (1) bath, (2) electrolyte, (3) treated sample, (4) stirrer, (5) thermometer, and (6) current source.

To determine the surface element composition, from three to five areas of a size of 300 × 200 μm² were scanned. The depth of penetration of the probing beam was 2–5 μm, depending on the coating material. The obtained element-composition data were averaged.

2.5. Coating Wear-Resistance Measurements

Data on coating wear resistance were obtained using a laboratory-made installation simulating the end friction (Fig. 4). A counterbody (indenter) comprising a cylinder of a diameter of 2.3 mm made of fast-cutting steel of R6M5 grade was lowered onto the coating. The indenter was pressed to the sample with a pressure of 6.3 MPa. The sample with coating, under the effect of an electric motor, performed a reciprocal motion under the loaded indenter at an increment of 1 cm 30.7 times/min (Fig. 4) [3]. In the moment of coating wearing off, the indenter/coating/metal circuit electric resistance reduced dramatically. The coating wear resistance was estimated from the time passed from the test start to the moment of dramatic reduction of the electric resistance of the indenter–dielectric coating–base metal circuit.

2.6. Coating-Thickness and Roughness Measurements

The coating thickness was measured using a VT201 vortex-current thickness meter (Russia). The VT-201 thickness meter allows measurements to be taken of coating thicknesses from 2 to 1100 μm. Measurements of thickness were carried out at a random ten sites from each side of the sample, and the obtained data

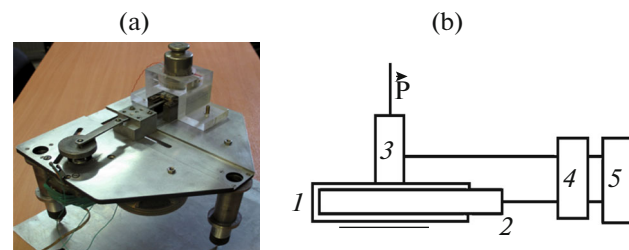


Fig. 4. (a) Laboratory installation for estimation of the coating wear resistance. Installation scheme: (1) coating, (2) metal, (3) indenter, (4) voltmeter operating in the resistance-measurement mode, and (5) recorder. (b) P is end load.

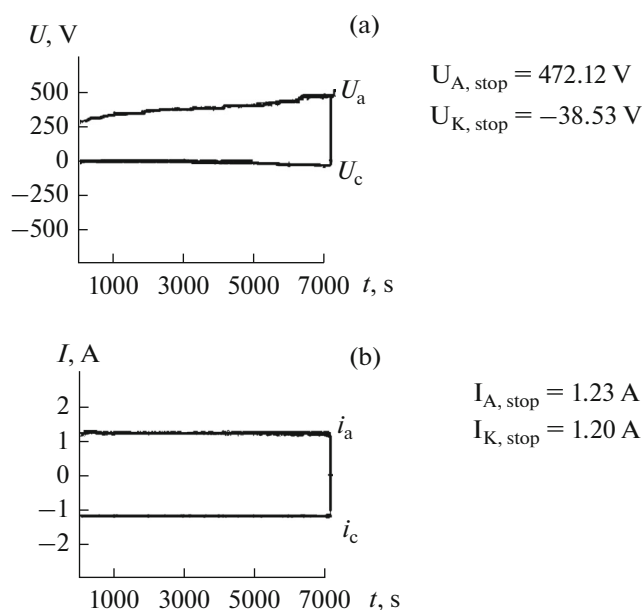


Fig. 5. Example of changes in (a) the voltage on electrodes and (b) currents upon anodic-cathodic treatment of the sample made of alloy of AMg5 grade in the silicate electrolyte over time.

were averaged. Roughness determination and construction of 3D images were carried out using a LEXT OLS3100 confocal scanning-laser microscope (Japan). Samples were studied and pictured at a resolution to 0.12 μm .

2.7. Microhardness Measurements

Measurements of sample microhardness were carried out using a DUH-W201 microhardness meter (Japan) from the depth of indenter penetration into the coating material under a load. A Berkovich diamond pyramid with an angle by the tip of 115° served as an indenter. The load on the indenter was equal to 0.5 N, while the depth of penetration here did not exceed 2 μm . The average microhardness value was calculated from five to ten measurements performed in randomly selected surface sites.

3. RESULTS AND DISCUSSION

3.1. Silicate Electrolyte

To obtain wear-resistant oxide coatings on aluminum and its alloys by the method of plasma electrolytic oxidation (PEO), an aqueous alkaline electrolyte containing liquid glass of some specific grade or silicate ($\text{Na}_2\text{SiO}_3 \cdot x\text{H}_2\text{O}$) with KOH or NaOH additives in different concentrations is extensively used in practice worldwide [2, 11, 14, 24]. Usually, wear-resistant PEO coatings are formed in anode-cathode modes at treatment durations of up to 2 h. An alternate current

with the commercial frequency of 50 Hz is used. Otherwise, one can use special current modes with different frequencies and ratios between the anode (I_a) and cathode (I_c) currents (I_a/I_c) from 0.9 to 1.2. In our experiments, coatings on samples were obtained similarly to the data of [6, 25, 26], where processes of growth and compositions and properties of coatings formed in borate electrolytes were investigated. The form of the anode-cathode current passed through the bath was as follows: $\tau_a = \tau_c = 0.02$ s, $i_a = i_c = 0.15$ A/cm², ratio $i_a/i_c = 1$, and treatment duration of 120 min. Electrolyte no. 2 of the composition 10 g/L $\text{Na}_2\text{SiO}_3 \cdot 9\text{H}_2\text{O} + 2$ g/L KOH was used.

Figure 5 shows the data on changes in the voltage on electrodes of (a) and (b) currents passed through the bath under treatment of a sample of a size of $10 \times 40 \times 1$ mm³ or of a surface area of ~ 8 cm² over time. It is seen that, at constant values of $i_a = i_c$ (Fig. 5b), one observes a gradual increase of the voltage on electrodes at anodic (U_a) or cathodic (U_c) polarization of the sample under treatment. Here, $U_a = f(t)$ is not symmetric to $U_c = f(t)$. At the same specific moment, $U_a \gg U_c$. The latter is usual for anode-cathode formation and related to the fact that, during the anode period, the ionic current is predominant and yields an increase in the coating thickness, while, in the cathode period, the electronic current is predominant. It is generally accepted that electric-spark and arc discharges are absent during the cathode period, whereas the electronic current flowing through the growing coating heats up the internal part of the growing oxide layer, thus promoting the transformation of low-temperature oxide phases into high-temperature ones. The parameters of the produced coating are shown in Table 2. The coating on alloy of grade AMg5 contains an expressed crystalline phase of $\gamma\text{-Al}_2\text{O}_3$.

Figure 6 shows images of the surface of coatings obtained using a microprobe analyzer (a, b). The surface of coatings is heterogeneous and consists of molten formations that must have emerged under effect of electric discharges due to the formation of micromelts and their fast cooling down to the electrolyte temperature. A similar appearance of the coating surface was obtained using a confocal laser microscope (Fig. 7).

According to the data of microprobe analysis, the composition of the surface part of coatings (up to 5 μm) was (at %) 58.5 O, 1.4 Na, Al 28, 1.9 Mg, 9 Si, and 1.3 K. Thus, the coatings consist of aluminum, silicon, and magnesium oxides. In other words, the coatings contain oxides of elements of both treated alloy (Al, Mg) and electrolyte (Si, Na, K).

Tests of coating wear resistance performed using a laboratory installation at an indenter load of 6.3 MPa demonstrated that it was impossible to wear the coating down to the base within 2 h under the above conditions.

Table 2. Thickness h , microhardness H , roughness factor R_a , and phase composition of coating formed on alloy of grade AMg5 in silicate and borate electrolytes

Electrolyte, g/L	U_a , V	T , °C	h , μm	H , MPa	Phase composition	R_a , μm
$\text{Na}_2\text{SiO}_3 - 10$ $\text{KOH} - 2$	472.1	13	88 ± 3	2091.2	$\gamma\text{-Al}_2\text{O}_3$	3.06
$\text{K}_2\text{B}_4\text{O}_7 - 20$	550.7	28	63 ± 4	15850	$\gamma\text{-Al}_2\text{O}_3$	4.43

U_a and T °C are the final voltage on the bath and electrolyte temperature upon the treatment-process completion, respectively.

Thus, the coatings formed in the silicate electrolyte are in compliance with the literature data with respect to main characteristics (thickness, phase composition, wear resistance, and element composition).

3.2. Borate Electrolyte

For the study, borate electrolyte no. 1 of the composition $20 \text{ g/L K}_2\text{B}_4\text{O}_7 \cdot 4\text{H}_2\text{O}$ [6, 25] was used. As in the case of a silicate electrolyte, an anodic–cathodic current was used: $\tau_a = \tau_c = 0.02 \text{ s}$, $i_a = i_c = 0.15 \text{ A/cm}^2$, ratio $i_a/i_c = 1$, and treatment duration of 120 min.

Figure 8 shows the data on changes in the voltage on electrodes of (a) anode and (b) cathode currents passed through the bath at treatment of a sample or of a surface area of $\sim 24 \text{ cm}^2$ over time.

Unlike the process of coating formation in the silicate electrolyte, here, the formation voltage during the anodic half-period (U_a) attains the maximal value as early as within 3000 s – it is then maintained by the current source ($\sim 530 \text{ V}$). In view of this, reduction of the anodic current (i_a) is observed after 3000 s. Such a behavior of voltage–current values implies that the contribution of dissolution currents is noticeably smaller in the borate electrolyte than in the silicate–alkaline one. In other words, in both cases, coatings are formed under somewhat different conditions.

Moreover, one can suggest that application of current sources with higher values of anodic voltage will allow producing coatings of larger thicknesses and better wear-resistance characteristics.

The coatings are fairly well crystallized (see Fig. 9). In both electrolytes, coatings with the $\gamma\text{-Al}_2\text{O}_3$ phase were produced on the aluminum alloy of AMg5 grade, whereas coatings containing the γ - and $\alpha\text{-Al}_2\text{O}_3$ phases (with predominance of $\alpha\text{-Al}_2\text{O}_3$) were produced on the alloy of D16 grade. The element composition of coatings obtained on the alloy of the AMg5 grade in the borate electrolyte was (at %) 59.9 O, 1.9 Mg, and 38.2 Al. Unlike coatings formed in the silicate electrolyte, those obtained in the borate electrolyte do not contain compounds of electrolyte components (B, K). In other words, coatings formed in the borate electrolyte consist predominantly of aluminum oxides.

The thickness of coatings formed on the aluminum alloys of the AMg5 grade is $63 \mu\text{m}$ that is smaller than that of coatings formed in the silicate electrolyte ($88 \mu\text{m}$), but the obtained samples are characterized with a noticeably higher microhardness of the external layer than those obtained in the silicate electrolyte (15850 and 2091 MPa, respectively; see Table 2). Coatings wear-resistance tests showed, that under the above conditions, it was impossible to wear off the coating produced in the borate electrolyte on the alloy of AMg5 grade until the base within 2 h.

As in the case of a silicate electrolyte (Figs. 6, 7), the coating surface is heterogeneous and consists of molten structures that must emerge under effect of electric discharges due to formation of micromelts and their fast cooling to the electrolyte room temperature (Fig. 10).

A series of conclusions can be made from comparison of the regularities of formation and properties of wear-resistant coatings produced by the PEO method in borate (No. 1) and silicate (No. 2) electrolytes: (1) in the borate electrolyte, the contribution of dissolution currents is much smaller in the process of coating formation than in the silicate electrolyte; (2) unlike the coatings formed in the silicate electrolyte (with noticeable presence of electrolyte components, for instance, silicon), those obtained in the borate electrolyte consist predominantly of aluminum oxides and are crystallized to a larger degree in comparison with those obtained in the silicate electrolyte; (3) the thickness of coatings formed in the borate electrolyte is smaller than that of coatings obtained in the silicate electrolyte; and (4) the coatings formed in the borate electrolyte have a more developed surface and signifi-

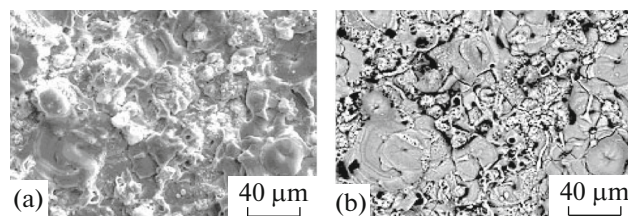


Fig. 6. SEM images of the surface of PEO coatings on alloy of AMg5 grade formed in the silicate electrolyte in (a) amplitude and (b) phase representations.

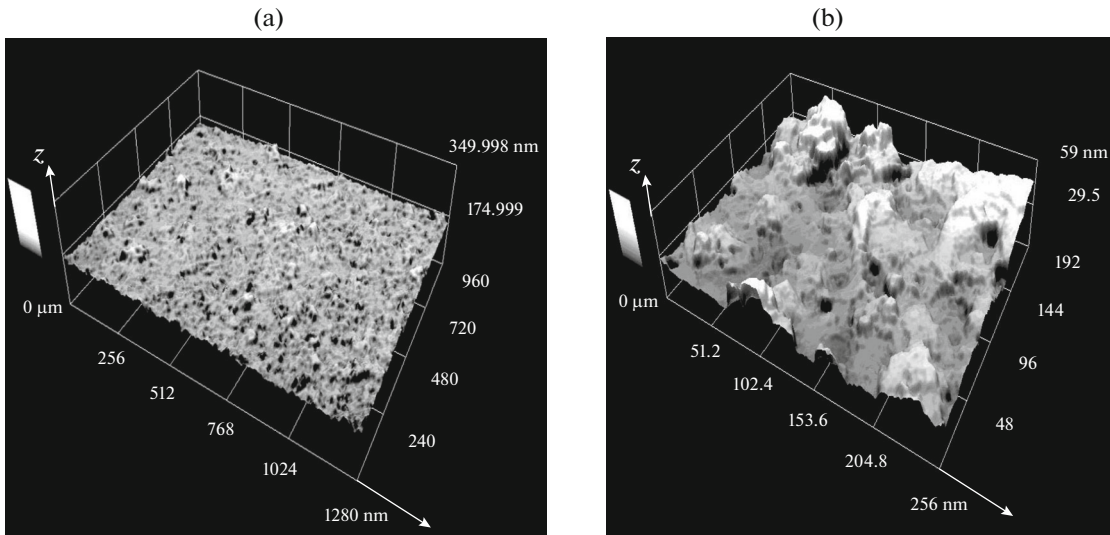


Fig. 7. Appearance of the surface of silicate coatings on alloy of AMg5 grade obtained using a confocal laser microscope at different magnifications.

cantly higher microhardness than those obtained in the silicate electrolyte (15850 and 2091 MPa, respectively). The coatings formed in both electrolytes are comparable with respect to wear-resistance properties (from wear-off duration under experimental conditions).

3.3. Mixed Borate–Silicate Electrolytes

It appears of interest to reveal whether the coatings formation in mixed borate–silicate electrolytes will yield a synergetic improvement of useful wear-resistance properties. The effect of the composition of the

mixed electrolyte on the properties of the coating on the aluminum alloys of AMg5 grade (microhardness of the external layer, thickness, and element and phase compositions) was studied. For this purpose, base

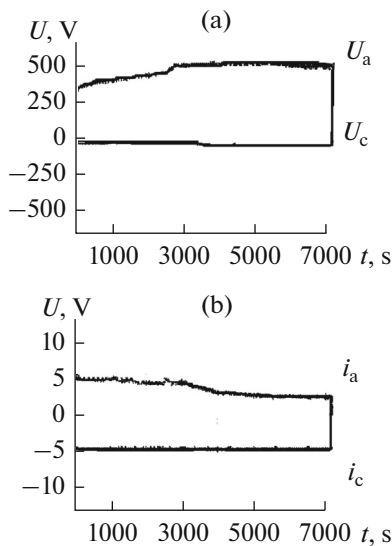


Fig. 8. Example of changes in (a) the voltage on electrodes and (b) currents upon anodic–cathodic treatment of the sample made of alloy of AMg5 grade in the borate electrolyte over time.

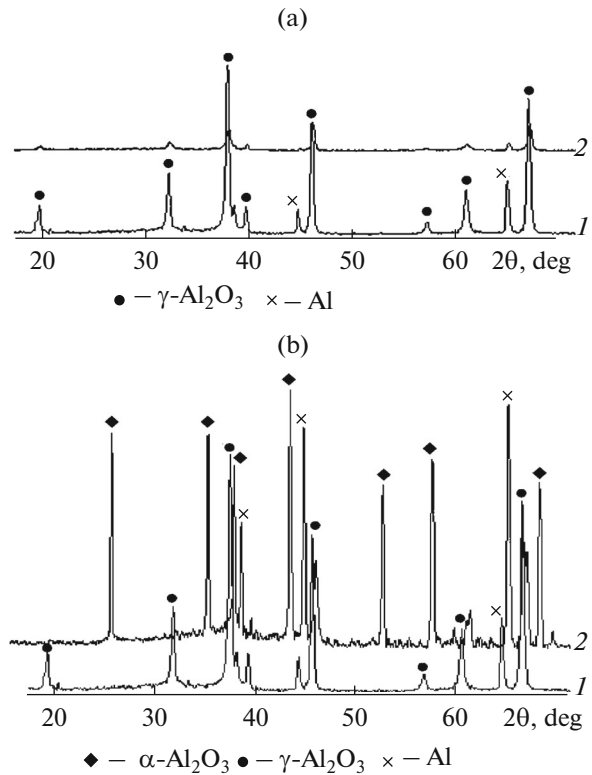


Fig. 9. (a) Phase composition of coatings obtained on aluminum alloy of AMg5 grade: (1) in the borate electrolyte, (2) in the silicate electrolyte; (b) on aluminum alloys of grades (1) AMg5 and (2) D16 in the borate electrolyte.

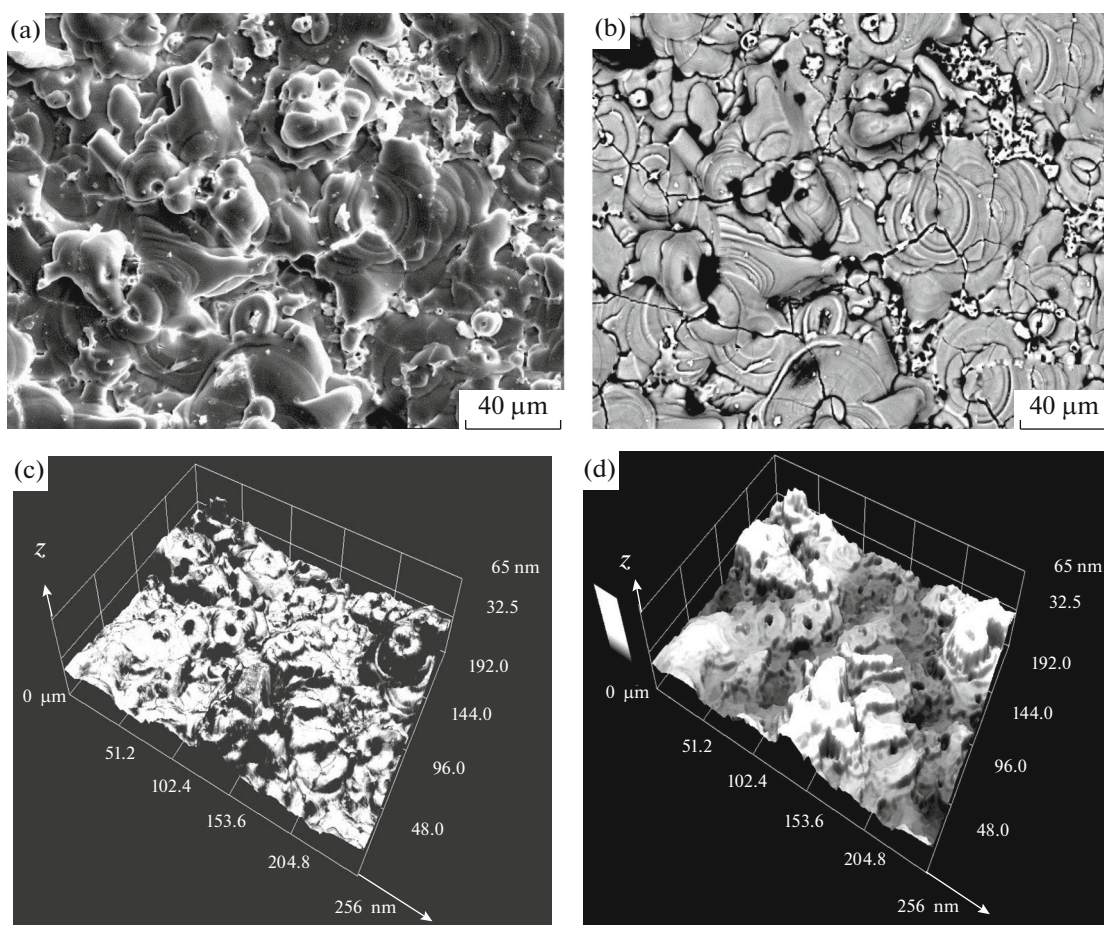


Fig. 10. Morphology of the surface of coatings formed on alloy of AMg5 grade in the borate electrolyte: (a, b) images obtained using a microprobe in (a) amplitude and (b) phase modes; (c, d) images obtained using a confocal microscope.

electrolytes (20 g/L $K_2B_4O_7$ and 10 g/L $Na_2SiO_3 \cdot 9H_2O + 2$ g/L KOH) were mixed at different volume ratios: 1 : 3, 1 : 1, and 3 : 1. As before, the anodic–cathodic current was used: $\tau_a = \tau_c = 0.02$ s, $i_a = i_c = 0.15$ A/cm², ratio $i_a/i_c = 1$, and treatment duration of 120 min.

With excess borate electrolyte ($m = 3 : 1$), changes in voltage and current values over time are similar to those in coating formation in the base borate electrolyte (Fig. 8). At an increase of the silicate–electrolyte content in the borate one ($m = 1 : 3$), changes in the voltage on the electrodes becomes similar to the behavior of this parameter as in the case of coating production in the base silicate electrolyte (Fig. 5).

When mixing base electrolytes at volume ratios $m = 1 : 1$ and $1 : 3$ (transition to an excess of silicate electrolyte in the mixed solution), turbid colloid solutions are formed. Thereafter, upon treatment of the first sample, solutions are transformed into a gel-like state over time, which complicates treatment of subsequent samples in them. This is most clearly seen for the mixed electrolyte with $m = 1 : 1$. The solution is trans-

formed into a gel-like state, and water-binding gel-like borosilicates are formed in the bulk. Figure 11 shows changes in voltages on electrodes and anodic and cathodic currents flowing upon the formation of the first coating in the electrolyte with $m = 1 : 1$, prior to its transformation into gel. One can see that, in this case, changes in voltages on electrodes are substantially different from the behavior of this parameter in base electrolytes. The total electric-power expenditures are much lower. Also, the thickness of the formed coating is noticeably smaller than in base electrolytes (Fig. 12). Interestingly, here, the measured microhardness of the coating external layer in this very site does not have general monotonous changes in this parameter during electrolyte-composition variation (Fig. 13).

Table 3 summarizes the studied parameters of coatings formed in base borate and silicate electrolytes and the first samples in mixed borate–silicate electrolytes. Pits that are probably formed under the effect of electric breakdown with low mobility in solutions with high or increasing upon gel-formation viscosity are

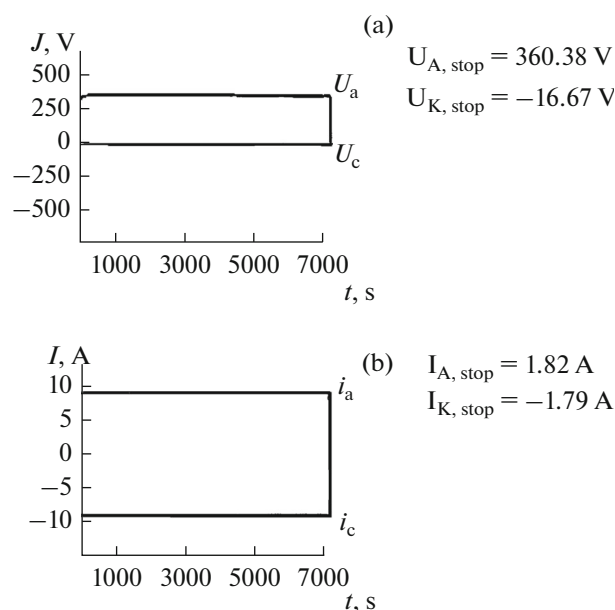


Fig. 11. Example of changes in (a) the voltage on electrodes and (b) anodic and cathodic currents under treatment of the first sample made of alloy of AMg5 grade in the mixed borate–silicate electrolyte over time.

observed on the surface of coatings with $m = 1 : 1$ and $1 : 3$.

As follows from the obtained data, general trends of changes in many parameters under study (thickness, roughness, surface relief, element composition, etc.) are not preserved in the area of structuring of the borate–silicate electrolyte (gel formation). At the same time, one observes monotonous changes in the value of microhardness of the external layer (no dramatic changes in microhardness take place, Fig. 13). This latter fact, in addition to the small thickness of the formed coatings ($\sim 30 \mu m$, Fig. 12) and their relatively low roughness ($0.9 \mu m$, Table 3), makes such coatings attractive for practical application. However, due to electrolyte structuring (gel formation), as early as after formation of the first coating, it becomes virtually impossible to further form coatings in the same solution by the PEO method. It is for this reason that it is of interest to test the effect of dilution of such an electrolyte by water or reduction of concentration of components (i.e., preventing the structuring processes) on formation of oxide coatings by the PEO method and their characteristics. Such coatings should provide interesting protective properties.

CONCLUSIONS

To sum up, the following conclusions can be drawn based on studies of coatings formed on aluminum alloys in silicate and borate electrolytes and during gradual replacement of a borate electrolyte by a silicate one:

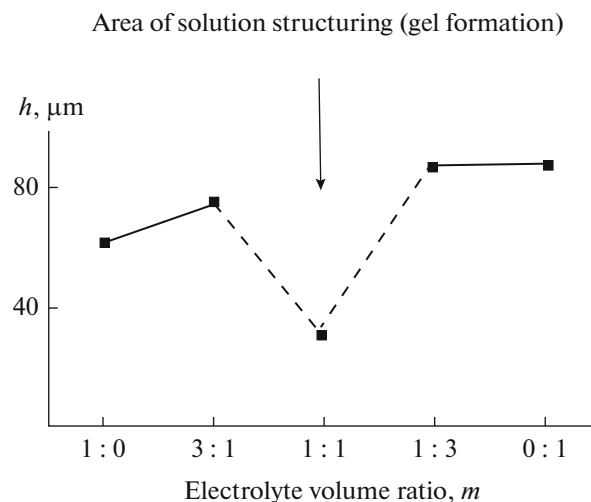


Fig. 12. Effect of the volume ratio (m) in borate–silicate electrolytes on the thickness of the formed coatings.

1. Of all the studied PEO coatings formed on alloy of AMg5 grade in borate, silicate, and mixed borate–silicate electrolytes, the most expressly crystallized is the coating formed in the borate electrolyte. Addition of the silicate electrolyte to the borate one results in reduction of the heights of reflections of the $\gamma\text{-Al}_2\text{O}_3$ phase in coatings.

2. The microhardness of the coatings' external layer gradually decreases upon transition from the borate electrolyte to the silicate one.

3. At a silicate–borate electrolyte ratio of $1 : 1$, upon formation of the first coating layer, one observes the process of electrolyte structuring: formation of borosilicates in the form of a viscous gel. Since the formed first coatings are characterized with small thickness and roughness at significant microhardness of the external layer, it appears of interest to study the effect of suppression of gel formation in the electrolyte (introduction of the third component, changes in the

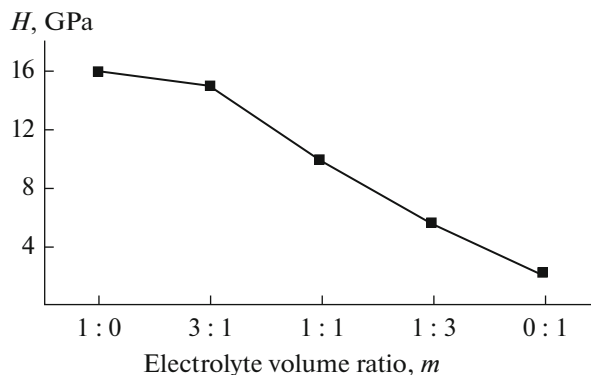


Fig. 13. Effect of the volume ratio (m) in borate–silicate electrolytes on the value of microhardness of the external layer of the formed coatings.

Table 3. Parameters of coatings on alloy of grade AMg5 formed in base borate and silicate electrolytes and first samples in mixed borate–silicate electrolytes

Electrolyte	m	U_c , V	h , μm	H , MPa	Phase composition	R_a , μm	Coating appearance
$\text{K}_2\text{B}_4\text{O}_7 - 20 \text{ g/L}$	1 : 0	550.7	62.5	15850	$\gamma\text{-Al}_2\text{O}_3$	4.4	Light, homogeneous
$\text{K}_2\text{B}_4\text{O}_7 + \text{Na}_2\text{SiO}_3 + \text{KOH}$	3 : 1	521.1	75.2	15018.7	$\gamma\text{-Al}_2\text{O}_3$	3.1	Light, homogeneous
$\text{K}_2\text{B}_4\text{O}_7 + \text{Na}_2\text{SiO}_3 + \text{KOH}$	1 : 1	360.4	29.6	10319.9	$\gamma\text{-Al}_2\text{O}_3$	0.9	Light, with pits
$\text{K}_2\text{B}_4\text{O}_7 + \text{Na}_2\text{SiO}_3 + \text{KOH}$	1 : 3	498.0	88.8	5664.2	$\gamma\text{-Al}_2\text{O}_3$	3.8	Light, with pits
$\text{Na}_2\text{SiO}_3 - 10 \text{ g/L}$	0 : 1	472.1	88.5	2091.2	$\gamma\text{-Al}_2\text{O}_3$	3.1	Light, homogeneous
$\text{KOH} - 2 \text{ g/L}$							

m is the volume ratio of borate/silicate electrolyte in the mixed electrolyte, U_c is the final voltage on electrodes upon the process completion, h is the coating thickness, H is the microhardness of the coating external layer, and R_a is the coating roughness factor.

pH value, changes in the concentrations of components, temperature, etc.) on the regularities of formation and characteristics of the formed PEO coatings.

ACKNOWLEDGMENTS

The work was partially supported by the Program of Basic Research “Far East” and State program no. 265-2014-001.

REFERENCES

- Bakovets, V.V., Polyakov, O.V., and Dolgovesova, I.P., *Plazmenno-elektroliticheskaya anodnaya obrabotka metallov* (Plasma and Electrolytic Anode Processing of Metals), Novosibirsk: Nauka, 1991.
- Terleeva, O.P., Belevantsev, V.I., and Slonova, A.I., *Prot. Met.*, 2003, vol. 39, no. 1, p. 50.
- Gordienko, P.S. and Rudnev, V.S., *Elektrokhimicheskoe formirovanie pokrytii na alyuminii i ego splavakh pri potentsialakh iskreniya i proboya* (Electrochemical Formation of Coatings on Aluminium and its Alloys under Arcing and Breakdown Potentials), Vladivostok: Dal'nauka, 1999.
- Markov, G.A., Belevantsev, V.I., Terleeva, O.P., et al., *Vestn. Mosk. Gos. Tekh. Univ. im. N. E. Baumana, Ser. "Mashinost."*, 1992, no. 1, p. 34.
- Malyshev, V.N., Bulychev, S.I., Markov, G.A., et al., *Fiz. Khim. Obrab. Mater.*, 1985, no. 1, p. 82.
- Rudnev, V.S., Yarovaya, T.P., Nedozorov, P.M., et al., *Korrozi. Mater., Zashch.*, 2005, no. 6, p. 21.
- Gordienko, P.S., *Obrazovanie pokrytii na anodnopolyarizovannykh elektrodakh v vodnykh elektrolitakh pri potentsialakh proboya i iskreniya* (Formation of Coatings on Anode Polarized Electrodes in Aqueous Electrolytes under Arcing and Breakdown Potentials), Vladivostok: Dal'nauka, 1996.
- Markov, G.A. and Markova, G.V., USSR Inventor's Certificate no. 526961, 1976.
- Gruss, L.L. and McNeil, W., *Electrochem. Technol.*, 1963, vol. 1, p. 283.
- Dittrich, K., Krysmann, W., Kurze, P., and Schneider, H., *Cryst. Res. Technol.*, 1984, vol. 19, p. 93.
- Markov, G.A., Terleeva, O.P., and Shulepko, E.K., *Tr. - Mosk. Inst. Neftekhim. Gazov. Prom-sti. im. I. M. Gubkina*, 1985, no. 185, p. 54.
- Suminov, I.V., Belkin, P.N., Epel'fel'd, A.V., et al., *Plazmenno-elektroliticheskoe modifitsirovanie poverkhnosti metallov i splavov* (Plasma and Electrolytic Modification for Metal and Alloy Surfaces), Moscow: Tekhnosfera, 2011.
- Yerokhin, A., Nie, X., Leyland, A., et al., *Surf. Coat. Technol.*, 1999, vol. 122, p. 73.
- Chernenko, V.I., Snezhko, L.A., and Papanova, I.I., *Poluchenie pokrytii anodno-iskrovym elektrolizom* (Coatings Generation with the Help of Anode-Spark Electrolysis), Leningrad: Khimiya, 1991.
- Nikolaev, A.V., Markov, G.A., and Peshchevitskii, B.I., *Izv. Sib. Otd. Akad. Nauk SSSR, Ser. Khim. Nauk*, 1977, no.12 (5), p. 32.
- Jiang, B.L. and Wang, Y.M., in *Surface Engineering of Light Alloys: Aluminium, Magnesium and Titanium Alloys*, Dong, H., Ed., Oxford, Cambridge, New Delhi: Woodhead Publ., 2010, p. 110.
- Belevantsev, V.I., Terleeva, O.P., Markov, G.A., et al., *Prot. Met.*, 1998, vol. 34, p. 416.
- Rakoch, A.G., Dub, A.V., and Gladkova, A.A., *Anodirovanie legkikh splavov pri razlichnykh elektricheskikh rezhimakh. Plazmenno-elektroliticheskaya nanotekhnologiya* (Light Alloys Anodization under Different Electrical Conditions. Plasma and Electrolytic Nanotechnology), Moscow: Staraya Basmanaya, 2012.
- Rudnev, V.S., *Tsvetn. Met. (Moscow, Russ. Fed.)*, 2006, no. 11, p. 70.
- Rudnev, V.S., *Tekhnol. Legk. Splavov*, 2007, no. 2, p. 121.
- Rudnev, V.S., *Prot. Met.*, 2007, vol. 43, p. 275.
- Rudnev, V.S., *Prot. Met. Phys. Chem. Surf.*, 2008, vol. 44, p. 263.
- Markov, G.A., Slonova, A.I., and Terleeva, O.P., *Prot. Met.*, 1997, vol. 33, no. 3, p. 257.
- Petrovyants, A.A., Malyshev, V.N., Fedorov, V.A., and Markov, G.A., *Trenie Iznos*, 1984, vol. 5, p. 350.
- Rudnev, V.S., Yarovaya, T.P., Nedozorov, P.M., and Boguta, D.L., RF Patent 2263164, 2005.
- Li, X., Rudnev, V.S., Zheng, X.H., et al., *J. Alloys Compd.*, 2008, vol. 462, p. 99.

Translated by D. Marinin